Sheet Metal 2023 Materials Research Forum LLC
Materials Research Proceedings **25** (2023) 387-394 https://doi.org/10.21741/9781644902417-48

Dynamic conformity assessment for joining force monitoring using Bayes filters

Lorenz Butzhammer[1,a *], Fabian Kappe[2,b], Gerson Meschut[2,c] and Tino Hausotte[1,d]

[1]Friedrich-Alexander-Universität Erlangen-Nürnberg, Chair of Manufacturing Metrology (FMT), Nägelsbachstr. 25, 91052 Erlangen, Germany

[2]Laboratory for Material and Joining Technology (LWF), Paderborn University, Pohlweg 47-49, 33098 Paderborn, Germany

[a]Lorenz.Butzhammer@fmt.fau.de, [b]fabian.kappe@lwf.upb.de, [c]meschut@lwf.upb.de, [d]Tino.Hausotte@fmt.fau.de

Keywords: Metrology, Joining, Force

Abstract. Monitoring force-displacement or force-time curves is a widely used quality control technique in the field of mechanical joining. For online monitoring of self-piercing riveting, envelope curves are often used to define a tolerance zone for the measured setting force. However, the measurement uncertainty is typically not considered and the force curve of a joint can be wrongly rated as non-conform due to measurement errors and noise. In this article, we present a method for dynamical online filtering and uncertainty determination for noisy force curves using two types of Bayesian filters. The methodology is based on a Bayesian probability framework using a priori information for the process curve and sensor noise. To investigate the general feasibility of the method, force measurements with different noise levels are simulated and processed. The conformity is further assessed taking the uncertainty of the filtered signal into account. The results show that the Bayes filter technique is principally able to reduce noise for well-known characteristics of the process curve and sensor noise. Advantages over common filtering techniques, especially for experimental conditions with less known characteristics, are still to be verified. The methodology could be used in future for closed-loop controls to adapt process parameters dynamically.

Introduction

Mechanical joining is established in a variety of production processes in industry, i.e. in the automotive sector. Different joining processes such as self-piercing riveting (SPR) or clinching are increasingly adapted to further material combinations and process conditions. These processes are often used to join multi-material structures as thermal joining processes reach their process limits due to the different material properties. In case of SPR, a joint of two or more sheets is created using an auxiliary joining part (the rivet). The process generally consists of a punch, a blank holder, the rivet, the parts to be joined and the die (see Fig. 1). The process itself can be divided into four stages. First, the sheets are placed between the punch and the die and the blank holder fixes them. Subsequently, the rivet receives a feed from the punch and cuts through the punch-sided joining part. The joint is created by upsetting of the rivet in the die-sided sheet, which leads to a force and form fit connection. The process sequence and a typical force-displacement curve are shown schematically in Fig. 1.

To ensure a high load-bearing capacity of mechanical joints in series production, quality monitoring is important. On the one hand, quality-relevant parameters such as the interlock or the minimum die-side material thickness are measured. These can only be detected in macro sections, which leads to the destruction of the joint. On the other hand, a widespread non-destructive method to detect or prevent from failed joints is to record force-displacement or force-time curves.

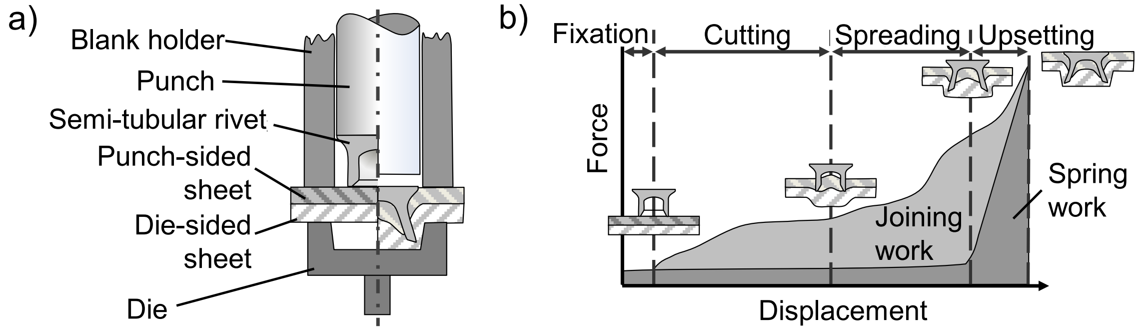

Fig. 1: Tooling for SPR and process sequence for SPR (a) as well as the exemplary joining force-displacement curve (b) according to [1].

In the case of self-piercing riveting, the guideline DVS/EFB 3410 [1] proposes two ways to rate if the force curve is in tolerance, window monitoring and tolerance monitoring. For the former method, 2D windows are defined in the force-displacement diagram that have to be crossed by the curve. This method is also used e.g. for clinch joining [2]. In case of tolerance monitoring, which considers the full process curve, envelope curves are defined as tolerance zone in which the measured curve must be located. In an on-line application, the process is stopped if the curve is out of tolerance. Several advantages such as reduced rejection rates can be achieved in this way.

In this article, we put a focus on tolerance monitoring. For this method, it is not fully clear how to define a proper tolerance band and how to consider the uncertainty of the measurement during on-line monitoring. Increased noise of the sensor can lead to a non-conformity decision although the process actually is in tolerance. Here, we investigate the use of recursive Bayesian filtering, taking a priori information about the process curve (assessed by experiments and statistical means) and about the measurement uncertainty into account. Bayesian filters can principally be used to dynamically correct (filter) incoming sensor readouts and estimate the uncertainty of the resulting filtered signal [3]. There are numerous application examples throughout different disciplines, such as GPS tracking [4], mobile robot localization [5] and dynamic coordinate measurements [6]. We use the Extended Kalman Filter (EKF) and a particle filter (PF) (see e.g. [9]), which are widely used and are able to handle nonlinear systems.

We investigate the performance of the filters for simulated measurements with different known noise levels, which represents an idealised case, but allows testing the general feasibility of the method. The conformity of the filtered measurements is finally rated using methods based on the internationally accepted Guide to the Expression of Uncertainty in Measurement (GUM).

Methodology

A rough summary of the methodology is given here before details are explained in the following subsections. The basic idea was to experimentally obtain a reference force-time curve (nominal curve) from repeated error-free joining events that can be used as a priori information for process measurements of future joining events. Experimental data is obtained by a self-piercing riveting process for two different material combinations. The a priori information is then fed to a Bayes filter for simulated sensor readouts, as well as the information of the known noise level. The experimentally obtained force-time curves are also used to define a conformity band around the reference curve. The filtered signal and its uncertainty is then used to judge if non-conformity can be stated, given a specified conformance probability.

Reference Curve and Tolerance Interval. The reference curves were generated by calculating mean curves from ten experimental joining events. In order to create the experimental data, self-piercing riveted joints were created using a specially developed joining system [8]. It was selected due to the open interfaces and the access to all data without internal prior filtering. The system is equipped with an inner and outer punch as well as a blank holder. In this investigation, only the inner punch as well as the blank holder were used to create the joints. The motion of the inner punch, with which the data required for the investigation are generated, is realised using a servo-electric drive. Joining forces of up to 80 kN and setting speeds of up to 80 mm/s can be realised in this way.

The maximum permissible error of the readout setting force values are given as ±0.5 % of the nominal force. The accuracy was verified with a load cell (HBM C6 R, F 04063), which was calibrated with a universal testing machine (Zwick Z100, accuracy class 0.5). However, the uncertainty of the load cell due to the calibration is in a similar range in comparison to the tested device, so the significance of the verification is limited. This is not seen as a problem as possible measurement errors are significantly lower than process variations and the simulated noise levels.

Two different sheet material combinations were used, aluminium for both sheets (Al-Al) and steel in combination with aluminium (St-Al). Consequently, two times ten curves were obtained and used for two different reference curves for the different material combinations. Due to the targeted application case of Bayesian online filtering with discrete time steps, force-time curves were used for this article. However, force-displacement curves were obtained as well and could also be used. The curves for the single measurements are shown in the left column of Fig. 2.

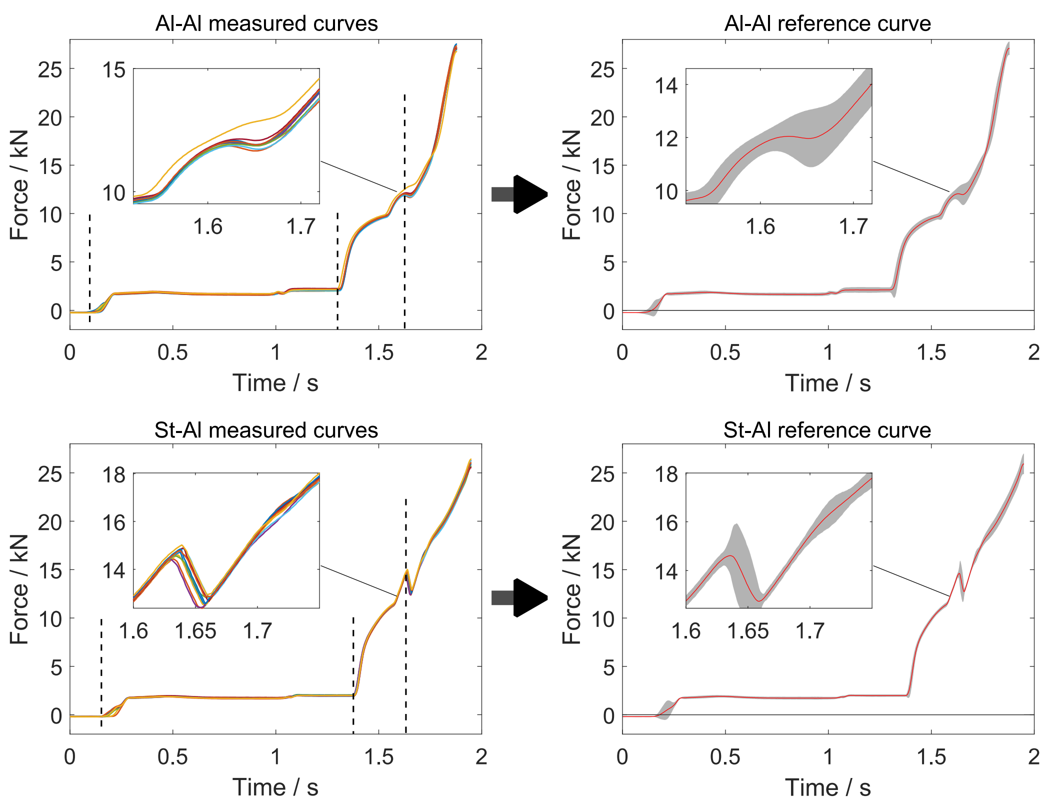

Fig. 2: Measured curves (left column) and calculated mean as reference curve (right column) with 99 % prediction interval (grey area) determined from the point-by-point empirical standard deviations.

The force monitoring shows a characteristic curve for the two investigated material combinations respectively. The first increase in force is caused by the application of the blank holder. The pneumatic drive keeps this force constant throughout the entire joining process. The second increase in force is attributed to the penetration of the rivet into the punch-sided joining part. Since the aluminium material has a greater overall thickness, the increase in force occurs a little earlier considering this joint. The force increases constantly until the punch-sided joining part is cut. This can be detected in the slight drop of the curves (see Fig. 2, detail). In the case of the multi-material joint, the cutting phase can be detected clearly. Due to the softer aluminium material, this is less pronounced in the Al-Al joint. Furthermore, a higher force is required for punching through the steel joint part than the aluminium joint part. The cutting phase is followed by a constant increase in the joining force. In this process phase, the interlock is formed. After the maximum is reached and the joint is embossed, the punch and the blank holder return to their initial position and the joint can be removed from the die.

For data post-processing, the ten single curves respectively were synchronised and resampled with a time step of 10 ms. In principle, this leads to an additional uncertainty contribution. As the observed influence was low compared to the process variation, this contribution was however not considered for the calculation of the tolerance interval. For each point in time, the arithmetic mean was used to extract a reference curve for the process (right column of Fig. 2). Approximating an underlying normal distribution, we additionally calculated the 99 % prediction interval (significance level α = 0.01) for single force values using the empirical standard deviation at each point in time, multiplied with the value of the Student's t-distribution $t = 3.25$ for $\nu = n - 1 = 9$ degrees of freedom and a probability of $1 - \alpha/2$. This prediction interval was used as tolerance interval for our later investigations.

Simulation of Noisy Force Curves. For the investigations in this article, we simulated noisy sensor readouts for each material combination starting with one of the ten curves obtained by experiment (see section Reference Curve and Tolerance Interval). A random number following a normal distribution $\mathcal{N}(0, \sigma_w^2)$ is added to each force value of this starting curve, simulating white noise. We used standard deviations of $\sigma_w = 0.1$ kN, $\sigma_w = 0.5$ kN and $\sigma_w = 1.0$ kN. In sum, the resulting simulated curves have an error component with regard to the reference curve due to the deviation of the underlying single curve from the mean curve (simulated process variation, which will be unknown to the filter) and a random error component according to the simulated readout noise.

Bayes Filter. Recursive Bayesian state estimation builds the theoretical background for the used filters. We give a short outline for the theory, which can be found in more detail e.g. in [9] and with respect to Bayesian tracking by means of PF in [10]. In case of a Markov process, the current state of a process only depends on its previous state, which can be expressed for discrete time steps by a process equation

$$\boldsymbol{x}_n = \boldsymbol{f}_{n-1} (\boldsymbol{x}_{n-1}, \boldsymbol{v}_{n-1}), \tag{1}$$

where $\boldsymbol{x}_n$ is the state vector at time step n and $\boldsymbol{f}_n$ the state transition function, which also depends on the process noise $\boldsymbol{v}$ [10]. In our case, the state space is one-dimensional, consisting of the setting force as a single parameter and the state transition is simply modelled by the force increment ΔF_{n-1} obtained from the reference curve. Therefore, we have $\boldsymbol{x}_n = F_n = F_{n-1} + \Delta F_{n-1 \to n} + v_{n-1}$. The measurements at each discrete point in time are accordingly given by

$$\boldsymbol{y}_n = \boldsymbol{h}_n(\boldsymbol{x}_n, \boldsymbol{w}_n), \tag{2}$$

where $\boldsymbol{w}_n$ is the measurement noise [10]. For our investigations, the most simple model of a direct measurement with additive white noise is used, i.e. $\boldsymbol{y}_n = F_n + w_n$.

The goal is now to estimate the current state in form of a posterior probability density function $p(\boldsymbol{x}_n\,|\boldsymbol{y}_{1:n})$, depending on all previous measurements, but in a recursive way. For this purpose, the following equation can be derived using Bayes law [10]:

$$p(\boldsymbol{x}_n\,|\boldsymbol{y}_{1:n}) \;=\; \frac{p(\boldsymbol{y}_\mathrm{n}|\boldsymbol{x}_\mathrm{n})\,p(\boldsymbol{x}_n|\boldsymbol{y}_{1:n-1})}{p(\boldsymbol{y}_n|\boldsymbol{y}_{1:n-1})}. \tag{3}$$

Eq. 3 represents the correction step for a Bayesian filter. The estimation of the current state based on all former measurements $p(\boldsymbol{x}_n|\boldsymbol{y}_{1:n-1})$ can be obtained from the Chapman-Kolmogorov equation [10]

$$p(\boldsymbol{x}_n\,|\boldsymbol{y}_{1:n-1}) \;= \int p(\boldsymbol{x}_\mathrm{n}|\boldsymbol{x}_{n-1})\,p(\boldsymbol{x}_{n-1}|\boldsymbol{y}_{1:n-1})\,\mathrm{d}\boldsymbol{x}_{n-1}. \tag{4}$$

It can be seen that Eq. 4 and 3 give the link between the posterior density function of the last step $p(\boldsymbol{x}_{n-1}|\boldsymbol{y}_{1:n-1})$ and the posterior density function of the current step $p(\boldsymbol{x}_n|\boldsymbol{y}_{1:n})$. First, the prediction (eq. 4) is done using the process model and then a correction according to eq. 3 is done using the current measurement.

The given equations represent a conceptual solution, but can generally not be solved analytically. For Gaussian distributions, the Kalman filter can be used in case of linear system equations and the extended Kalman filter (EKF) for non-linear systems by means of linearization [9]. Particle filters (PF) on the other hand are a class of sequential Monte Carlo methods, which can handle non-Gaussian distributions [10]. Particles representing possible process states are propagated and used to estimate a posteriori density function, which can in turn be used to get a state estimate and variance.

While the system equations of our model could generally be solved with a basic Kalman filter, we used the EKF and a PF to be able to implement models that are more complex in future. The implementation was done using the EKF and PF classes of the Control System Toolbox of Matlab R2020b (The MathWorks, Inc.). The process noise was roughly estimated with $\sigma_v = 0.01$ kN and given as input for the filters. In case of the measurement noise, the values used for the simulation were also passed to the filters. Both filter types were initialised with the first value of the reference curve. For the particle filter, 10^6 particles were used and initialised with a variance of $4\cdot\,\sigma_w$. A Gaussian measurement likelihood function was used. The state estimate was obtained by the sample mean after the correction step. The standard uncertainty of the filtered curve was obtained from the corrected state estimation error variance.

Conformity Assessment. Regarding conformity assessment, we used the methodology given in DIN EN ISO 14253-1 [11], which was originally developed with regard to geometric product specification. The method is based on the Guide to the expression of uncertainty in measurement (GUM) [12] and one of its supplements [13]. With regard to the discussed application of on-line monitoring, the task is to identify a curve progression that runs out of tolerance. In such a case, the joining process would be stopped. This should only be done if there is a sufficient probability that the force is not conform. Consequently, the measurement is tested for non-conformity. Considering the measurement uncertainty, the tolerance interval should be extended with guard bands to reach a certain probability of non-conformance [11]. For an assumed normal distribution, an extension factor (to be multiplied with the standard uncertainty) of 1.65 must be used to calculate the acceptance limits for a probability of non-conformance of 95 %.

To sum up, the Bayes filter is applied to reduce the measurement noise considering a priori knowledge. The estimated force values as an output of the filter are dynamically tested for non-conformity by checking if the filtered force value is out of the acceptance interval, which is formed by the tolerance interval plus guard intervals that depend on the estimated standard uncertainty of

Materials Research Proceedings **25** (2023) 387-394 https://doi.org/10.21741/9781644902417-48

the filtered signal. As the filters need a certain time to settle with a reduced uncertainty, the time span from $t = 0$ to $t = 0.1$ s was not considered for conformity assessment.

Results and Discussion

The simulated noisy measurements are shown in the left column of Fig. 3 for the material combination St-Al. The insets show zoomed-in views around the point where the cutting through the punch-sided sheet starts and the point where the punch-sided joining part is cut.

It can be seen that a noise level of $\sigma_w = 0.5$ kN and $\sigma_w = 1$ kN leads to a measured signal that distinctly exceeds the tolerance interval. It is even hard to identify the different stages of the piercing riveting process.

In the right column of Fig. 3, the filtered version of the measurement signal is presented. The extended Kalman filter was used for the figure, but throughout our investigations, the particle filter led to nearly identical results. This can be expected as Gaussian distributed noise was simulated and modelled. Differences would be expected if the probability distributions had major deviations from the Gaussian shape. Significant differences only exist in the starting phase up to around $t = 0.1$ s until the filters show a stable behaviour with small variance. As already mentioned in the previous chapter, the non-stable time span was excluded from conformity assessment. For the use in real applications, it should be ensured that the filter is stable at the onset of the joining process.

The zoomed-in views show that the filtered signal is close to the true values. It has to be emphasised that these true values deviate from the reference curve and were therefore not directly used as a priori information. In Fig. 3, the true curve is not in the centre of the tolerance interval, which was constructed symmetrically around the reference curve.

When the non-conformity evaluation is applied, it shows that all filtered curves are within the acceptance interval (also for the filtered Al-Al curves, which are not shown here). Non-conformity can therefore not be stated with a probability of 95 % or higher. This is the desired result as the noisy curves were simulated from a curve that was used to construct the tolerance interval. It should however be noted that using a different curve from the experimental repetitions as starting point for simulation could result in a different decision. For real applications, a greater tolerance interval might be used to cover acceptable variations from different process conditions. Long-term data and a comparison with other quality inspection techniques might be a sound basis for this, although the concrete implementation is an open question.

While we performed our simulations and data processing off-line, the method in principle can be used for real-time filtering. However, we did not evaluate run times and the real-time capability.

The investigated noise levels are higher than for typical sensor outputs from closed measurement systems used for self-piercing riveting. If the acceptable process variation is multiple times greater than the sensor noise, the achievable improvements due to the filtering might not be significant. Unknown systematic measurement errors might further deteriorate the results. A Bayesian framework could however be interesting in special applications, e.g. if information from multiple sensors has to be fused.

Materials Research Proceedings **25** (2023) 387-394 https://doi.org/10.21741/9781644902417-48

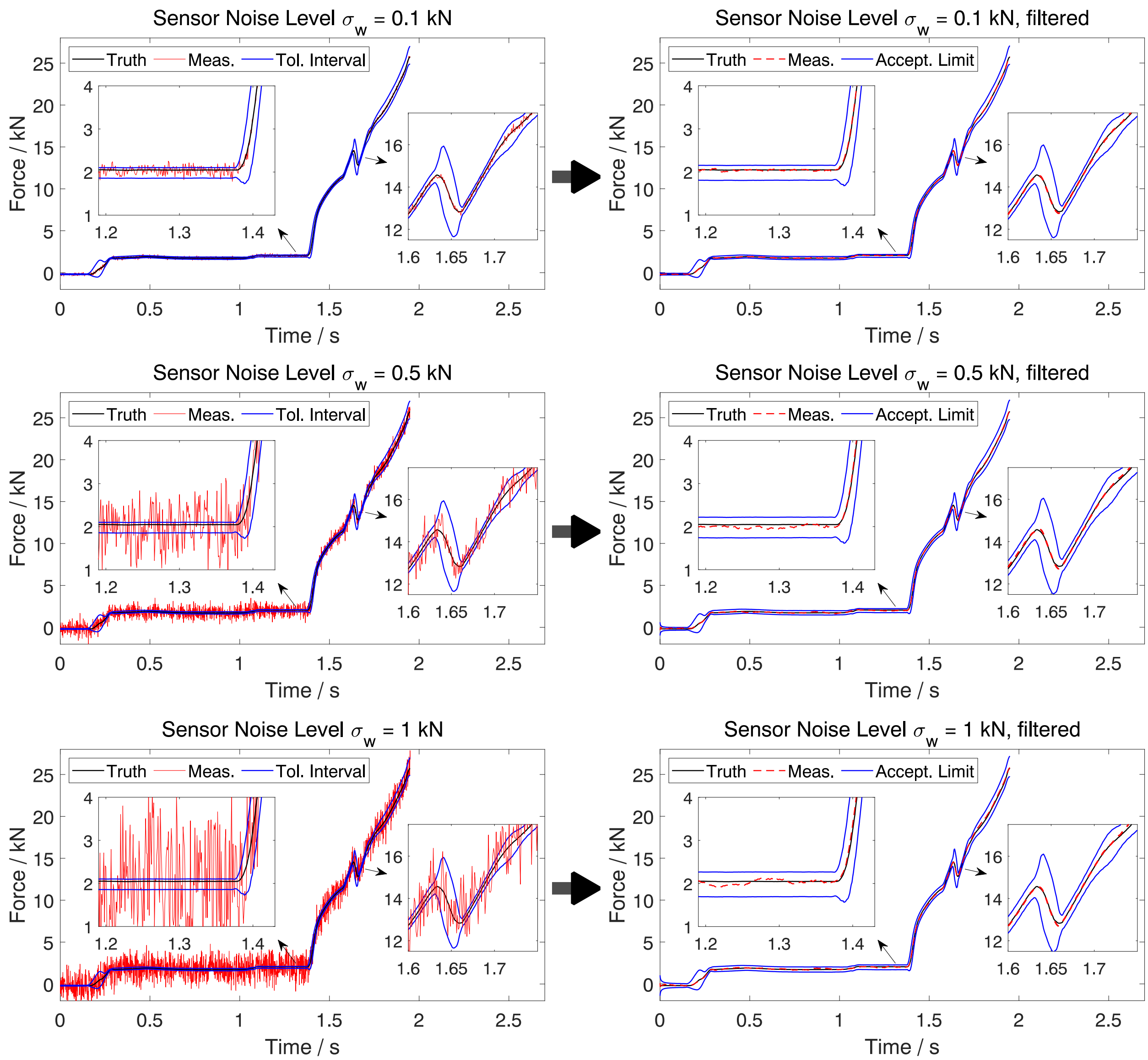

Fig. 3: Results for the material combination St-Al. Left: Simulated process curves with different noise level (red curve) and indicated tolerance interval (blue curves). Right: Filtered signal (extended Kalman filter, red curve) and indicated acceptance limits (Tolerance interval extended with guard bands that depend on the uncertainty output from the Kalman filter, blue curve) for a probability of non-conformance of 95 %.

Summary

In this article, a methodology to increase the accuracy of dynamic force measurements for mechanical joining by Bayesian filtering and to assess the conformity in the sense of quality monitoring, taking the measurement uncertainty into account is presented. A reference curve was statistically obtained from acceptable joints and used as a priori information for an extended Kalman filter and a particle filter. The filter performance was demonstrated by means of simulated measurements with different noise levels. It was shown that the measurement noise can effectively be reduced and the conformity properly assessed. The presented investigations should only be seen as a proof of principle that Bayes filters can theoretically be used to reduce noise and estimate the uncertainty for force-time or force-displacement curves obtained by mechanical joining. The noise levels investigated here do not represent typical conditions for commercial devices. For real applications, the behaviour and dependencies of sensors are additionally more complex and the noise characteristics as well as specific systematic errors are not necessarily known. The filter performance deteriorates the more the assumed characteristics of the sensors and of the process deviate from reality. This can even lead to results that are inferior to filters that rely on observation-only inference [14]. Regarding future work, it remains to be shown that the methodology is advantageous for real noisy data and is outperforming non-Bayesian filters. For joining processes and sensors that cannot be accurately characterised, there might be no improvement. However, for well-characterised systems, Bayesian filtering might be a useful technique for future application cases, where process parameters are dynamically adapted in a closed-loop control.

Acknowledgements
Funded by the Deutsche Forschungsgemeinschaft (DFG, German Research Foundation) – TRR 285 – Project-ID 418701707 - subprojects C02 and C05.

References

[1] DVS/EFB 3410, Stanznieten - Überblick, 2005.

[2] Y. Tan, O. Hahn, and F. Du, Process monitoring method with window technique for clinch joining, ISIJ International, vol. 45, no. 5, pp. 723–729, 2005. https://doi.org/10.2355/isijinternational.45.723

[3] S. Särkkä, Bayesian Filtering and Smoothing. Cambridge: Cambridge University Press, 2013. https://doi.org/10.1017/CBO9781139344203

[4] E. D. Kaplan and C. J. Hegarty, Understanding GPS: principles and applications. Artech House Publishers, 2005.

[5] S. Thrun, W. Burgard, and D. Fox, Probabilistic Robotics. The MIT Press, 2005.

[6] E. Garcia, T. Hausotte, and A. Amthor, Bayes filter for dynamic coordinate measurements - accuracy improvment, data fusion and measurement uncertainty evaluation, Measurement, vol. 46, no. 9, pp. 3737–3744, 2013. https://doi.org/10.1016/j.measurement.2013.04.001

[7] D. Simon, Optimal state estimation: Kalman, H [infinity] and nonlinear approaches. Hoboken, N.J: Wiley-Interscience, 2006. https://doi.org/10.1002/0470045345

[8] F. Kappe, S. Wituschek, M. Bobbert, and G. Meschut, Determining the properties of multi-range semi-tubular self-piercing riveted joints, Production Engineering, vol. 16, no. 2-3, pp. 363–378, 2022. https://doi.org/10.1007/s11740-022-01105-2

[9] A. J. Haug, Bayesian Estimation and Tracking. John Wiley & Sons, Inc., 2012. https://doi.org/10.1002/9781118287798

[10] M. S. Arulampalam, S. Maskell, N. Gordon, and T. Clapp, A tutorial on particle filters for online nonlinear/non-Gaussian Bayesian tracking, IEEE Transactions on Signal Processing, vol. 50, no. 2, pp. 174–188, 2002. https://doi.org/10.1109/78.978374

[11] DIN EN ISO 14253-1, Geometrische Produktspezifikationen (GPS) - Prüfung von Werkstücken und Messgeräten durch Messen - Teil 1: Entscheidungsregeln für den Nachweis von Konformität oder Nichtkonformität mit Spezifikationen (ISO/DIS 14253-1:2016), 2018.

[12] JCGM 100:2008, Evaluation of measurement data - guide to the expression of uncertainty in measurement, 2008.

[13] JCGM 106:2012, Evaluation of measurement data - the role of measurement uncertainty in conformity assessment, 2012.

[14] T. Li, J. M. Corchado, J. Bajo, S. Sun, and J. F. De Paz, Effectiveness of Bayesian filters: An information fusion perspective, Information Sciences, vol. 329, pp. 670–689, 2016. https://doi.org/10.1016/j.ins.2015.09.041